

# Dual Role for $\text{Zn}^{2+}$ in Maintaining Structural Integrity and Inducing DNA Sequence Specificity in a Promiscuous Endonuclease<sup>\*[5]</sup>

Received for publication, July 19, 2007, and in revised form, August 31, 2007. Published, JBC Papers in Press, September 4, 2007, DOI 10.1074/jbc.M705927200

Matheshwaran Saravanan<sup>†1</sup>, Kommireddy Vasu<sup>‡</sup>, Soumitra Ghosh<sup>‡</sup>, and Valakunja Nagaraja<sup>‡§2</sup>

From the <sup>†</sup>Department of Microbiology and Cell Biology, Indian Institute of Science, Bangalore 560 012, India and the <sup>§</sup>Jawaharlal Nehru Centre for Advanced Scientific Research, Bangalore 560 064, India

We describe two uncommon roles for  $\text{Zn}^{2+}$  in enzyme KpnI restriction endonuclease (REase). Among all of the REases studied, KpnI REase is unique in its DNA binding and cleavage characteristics. The enzyme is a poor discriminator of DNA sequences, cleaving DNA in a promiscuous manner in the presence of  $\text{Mg}^{2+}$ . Unlike most Type II REases, the active site of the enzyme comprises an HNH motif, which can accommodate  $\text{Mg}^{2+}$ ,  $\text{Mn}^{2+}$ , or  $\text{Ca}^{2+}$ . Among these metal ions,  $\text{Mg}^{2+}$  and  $\text{Mn}^{2+}$  induce promiscuous cleavage by the enzyme, whereas  $\text{Ca}^{2+}$ -bound enzyme exhibits site-specific cleavage. Examination of the sequence of the protein revealed the presence of a zinc finger CCCH motif rarely found in proteins of prokaryotic origin. The zinc binding motif tightly coordinates zinc to provide a rigid structural framework for the enzyme needed for its function. In addition to this structural scaffold, another atom of zinc binds to the active site to induce high fidelity cleavage and suppress the  $\text{Mg}^{2+}$ - and  $\text{Mn}^{2+}$ -mediated promiscuous behavior of the enzyme. This is the first demonstration of distinct structural and catalytic roles for zinc in an enzyme, suggesting the distinct origin of KpnI REase.

A large number of proteins have bound zinc ions, which contribute to protein stability and/or catalytic functions more widely than any other transition metal ions (1, 2). A catalytic role for zinc was first shown in the case of carbonic anhydrase (3), and its structural role was first proposed and demonstrated for the transcription factor TFIID (4, 5). Since then, the roles for  $\text{Zn}^{2+}$  in numerous zinc-binding proteins have been identified and characterized. In many examples, the role of zinc ion is neither strictly structural nor catalytic, as in aminoacyl-tRNA synthetases, where zinc is involved in amino acid discrimination (6). Zinc binding motifs are structurally diverse and are present among proteins that perform a broad range of functions in various cellular processes. For instance, the motifs play a role in DNA recognition, transcription activation, protein folding and assembly, and protein-protein interactions (7).

Zinc binding is observed in different groups of nucleases, I-PpoI, I-TevI, T4 endonuclease VII, DNA repair endonuclease IV, colicin E7, and S1 nuclease (8–12). The binding of zinc is important for structural stability of I-PpoI, I-TevI, and T4 endonuclease VII and for catalysis in endonuclease IV and colicin E7. Bioinformatic analysis showed that McrA has a zinc binding fold, suggested to be needed for structural integrity (13). R.BslI contains two glucocorticoid receptor-like zinc ( $\text{Cys}_4$ ) binding motifs, which are important for the protein-DNA and protein-protein interactions (14). In this paper, we describe two distinct roles for  $\text{Zn}^{2+}$  in R.KpnI.

Type II REases<sup>3</sup> require  $\text{Mg}^{2+}$  or a similar divalent metal ion to cleave DNA. Almost 3700 Type II restriction enzymes, representing more than 262 distinct specificities, are known to date (15). Most Type II REases belong to the PD... (D/E)XK superfamily (16). Recent structural and bioinformatics studies revealed that apart from the PD... (D/E)XK superfamily, few REases belong to other nuclease superfamilies, such as Nuc, HNH, and YIG-GIY, which are structurally unrelated to each other (17–19).

Sequence alignment and subsequent validation experiments showed that R.KpnI is the first member of the HNH superfamily (20). Although at first glance R.KpnI appeared to be a typical dimeric Type IIP REase recognizing and cleaving palindromic sequence GGTACC, it has several distinct features. The properties include prolific promiscuous activity in the presence of  $\text{Mg}^{2+}$  which is further enhanced with  $\text{Mn}^{2+}$ , efficient site specific high fidelity DNA cleavage when  $\text{Ca}^{2+}$  is used instead of  $\text{Mg}^{2+}$ , and suppression of the promiscuous cleavage activity in presence of  $\text{Ca}^{2+}$  (21). Kinetic studies revealed that the  $\text{Ca}^{2+}$ -mediated exquisite specificity is achieved at the step of DNA cleavage (22).

The alignment of McrA, T4 endonuclease VII, and R.KpnI is depicted in Fig. 1A. The former two enzymes have tetra-Cys  $\text{Zn}^{2+}$  fingers, whereas R.KpnI has an unusual CCCH putative  $\text{Zn}^{2+}$  finger. Here we describe the importance of the  $\text{Zn}^{2+}$  finger motif in  $\text{Zn}^{2+}$  coordination. Surprisingly, the bound  $\text{Zn}^{2+}$  has more complex, multiple roles in R.KpnI function, in a manner distinct from any other restriction-modification system.

## EXPERIMENTAL PROCEDURES

**Enzymes and DNA**—T4 polynucleotide kinase, Pfu DNA polymerase, and DpnI were purchased from New England Biolabs.

\* The costs of publication of this article were defrayed in part by the payment of page charges. This article must therefore be hereby marked "advertisement" in accordance with 18 U.S.C. Section 1734 solely to indicate this fact.

[5] The on-line version of this article (available at <http://www.jbc.org>) contains supplemental Fig. 1 and Table 1.

<sup>1</sup> Senior research fellow of the Council of Scientific and Industrial Research, Government of India.

<sup>2</sup> To whom correspondence should be addressed. Tel.: 91-80-23600668; Fax: 91-80-23602697; E-mail: [vraj@mcbl.iisc.ernet.in](mailto:vraj@mcbl.iisc.ernet.in).

<sup>3</sup> The abbreviations used are: REase, restriction endonuclease; WT, wild type.

Oligonucleotides (Sigma and Microsynth) were purified on 18% urea-polyacrylamide gel (33) and end-labeled with T4 polynucleotide kinase and [ $\gamma$ - $^{32}\text{P}$ ]ATP (6000 Ci/mmol).

**Mutagenesis, Expression, and Purification of Mutant Proteins**—The model of R.KpnI was built using the structure of T4 endonuclease VII and other structurally characterized HNH superfamily nucleases. The detailed procedure has been described and discussed previously (20). Site-directed mutagenesis was performed by the megaprimer method (23). The mutations were confirmed by sequencing. The WT and mutants were expressed in *Escherichia coli* BL26 ( $F^-$  omp T hsdSB (rB $^-$  mB $^-$ ) gal dcm  $\Delta$ lac (DE3) nin5 lac UV5-T7 gene 1) containing KpnI methyltransferase, and the cells were induced with 0.3 mM isopropyl- $\beta$ -D-thiogalactopyranoside as described previously (24). Cells were lysed by sonication in buffer A containing 10 mM potassium phosphate (pH 7.0), 1 mM EDTA, 7 mM 2-mercaptoethanol. The supernatant was subjected to 0–50% ammonium sulfate fractionation. The samples were dialyzed against buffer A and purified by phosphocellulose and Hi-Trap heparin columns. The fractions containing the enzyme were pooled and dialyzed against buffer B (10 mM Tris-HCl (pH 7.4), 0.1 mM EDTA, 50 mM KCl, 5 mM 2-mercaptoethanol, and 50% glycerol). The concentration of the proteins was estimated by the method of Bradford (25).

**Atomic Absorption Analysis**—Purified R.KpnI (10 mg) was denatured and renatured in the presence or absence of 100  $\mu\text{M}$   $\text{ZnCl}_2$  or 5 mM EDTA and then dialyzed overnight against 20 mM Tris-HCl (pH 7.4), 150 mM NaCl at 4 °C with buffer changes to eliminate excess metal ions or chelators. Chelex-100 resin (Sigma) was used to remove trace metal ions in all of the buffers. The samples were analyzed by atomic absorption spectroscopy. The dialyzed buffer after Chelex treatment was used as a blank, and the residual  $\text{Zn}^{2+}$  background was subtracted from the measurement of protein samples.

**$\text{Zn}^{2+}$  Blotting Assay**—Purified R.KpnI and its mutants (0–6  $\mu\text{g}$ ) was slot-blotted onto nitrocellulose membrane presoaked in buffer (10 mM Tris, pH 7.5, 100 mM NaCl, 1 mM EDTA). Proper transfer was ascertained by Ponceau-S staining with transferred protein amounts estimated using Quantity One software. After transfer, the membrane was incubated at 37 °C for 1 h in buffer containing 10 mM Tris-HCl, pH 7.5, 100 mM NaCl, 10 mM  $\text{MgCl}_2$  and subsequently washed three times (15 min each) in the same buffer. The membrane was next incubated in buffer containing 30  $\mu\text{Ci}$  of  $^{65}\text{ZnCl}_2$  (specific activity, 800 mCi/g; BARC, Mumbai) at room temperature for 1 h with gentle rocking. The unbound radioactivity was removed by washing the membrane three times with buffer (20 min each). The membrane was dried and exposed to a PhosphorImager screen.

**Electrophoretic Mobility Shift Assay**—Different concentrations of the WT (1–10 nM) and mutant R.KpnI (10–100 nM) were incubated with the 0.2 pmol of end-labeled double-stranded oligonucleotide (20-mer) containing the R.KpnI recognition site in binding buffer (20 mM Tris-HCl (pH 7.4), 25 mM NaCl, and 5 mM 2-mercaptoethanol) for 15 min on ice. The free DNA and the enzyme-bound complexes were resolved by 8% native polyacrylamide gel electrophoresis in 1 $\times$  TBE buffer (89

mM Tris-HCl, 89 mM boric acid, and 1 mM EDTA), and then signals were detected by autoradiography.

**In Vitro DNA Cleavage and Steady-state Kinetic Analysis**—Purified R.KpnI and its mutants were incubated with 500 ng of plasmid DNA in buffer containing 10 mM Tris-HCl (pH 7.4), 5 mM 2-mercaptoethanol, 2 mM  $\text{MgCl}_2$ , or 10–100  $\mu\text{M}$   $\text{ZnCl}_2$  for 1 h at 37 °C. The cleavage products were analyzed on 1% agarose gel. For kinetic analysis, the purified enzyme was dialyzed against 10 mM EDTA to remove any bound metal ions. Steady-state kinetic time courses with canonical DNA substrates were measured at DNA concentrations of 5–150-fold molar excess over dimeric enzyme (1 nM) in the presence of 100  $\mu\text{M}$   $\text{Zn}^{2+}$ . The kinetic parameters were determined as described (22).

**Circular Dichroism**—The wild type R.KpnI and its mutants harboring the C119A, C128A, C171A, and H174A mutations were analyzed by CD. The CD spectra were recorded at 25 °C from 250 to 200 nm using a JASCO J-720 spectropolarimeter and a cuvette of path length 0.2 cm. The spectra were collected at scanning rate of 50 nm/min, and triplicate spectrum readings were collected per sample. All of the samples were base line-corrected before calculations. The buffer used was 50 mM Tris-HCl (pH 7.4), 75 mM NaCl, 1 mM 2-mercaptoethanol. The proteins were at a concentration of 0.2  $\mu\text{g}/\mu\text{l}$ , and the molar ellipticity ( $\theta$ ) was calculated using the equation,

$$\theta = \frac{\theta_{\text{obs}} \times 10^{-3} \times M_r}{C \times l \times n \times 10^{-2}} \text{ deg dmol}^{-1} \text{ cm}^2 \quad (\text{Eq. 1})$$

where  $\theta_{\text{obs}}$  is the observed ellipticity,  $M_r$  is molecular weight,  $C$  is concentration (in mg/ml),  $l$  is the path length of the cuvette in centimeters,  $n$  refers to the number of residues, and deg is degrees. Thermal stability of the protein samples was assessed using CD by following changes in the spectrum with increasing temperature (25–75 °C). A single wavelength (222 nm) was chosen to monitor the protein structure, and the signal at that wavelength is recorded continuously as the temperature is raised.

**Tryptic Digestion of R.KpnI**—Proteolytic digestions of different samples of R.KpnI and its mutants (1 mg/ml) were carried out in 50 mM Tris-HCl buffer, pH 8.5, and at 37 °C using 1% trypsin. 5- $\mu\text{l}$  samples (5  $\mu\text{g}$ ) were taken after various time periods, and trypsin was inactivated with buffer containing phenylmethylsulfonyl fluoride. Samples were analyzed by 15% SDS-PAGE.

## RESULTS

**R.KpnI Has Two  $\text{Zn}^{2+}$  Binding Sites**—Sequence analysis and homology modeling of R.KpnI predicted the presence of an unusual CCCH zinc finger motif (20) different from other previously described commonly found zinc finger motifs (CCCC, CCHH, CCHC). The putative zinc-coordinating residues are shown in the model (Fig. 1B). The arrangement of cysteines and histidine (CCCH) in R.KpnI is rare among zinc finger proteins of prokaryotic origin. To estimate the bound  $\text{Zn}^{2+}$ , we performed atomic absorption spectrometry (Table 1). Extensively dialyzed R.KpnI was found to bind 2 mol of  $\text{Zn}^{2+}$ /mol of dimer. The dimeric nature of the enzyme has been established before

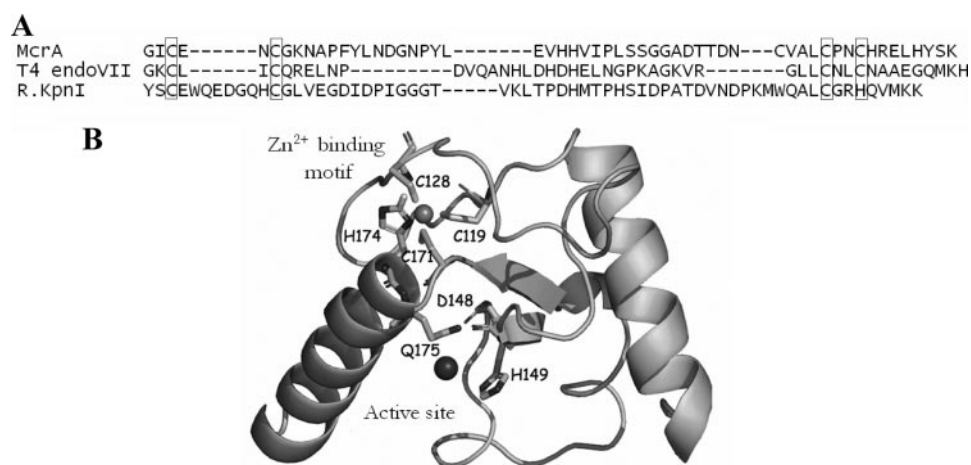


FIGURE 1. **R.KpnI zinc finger.** A, sequence alignment of McrA, T4 endonuclease VII, and R.KpnI. The Zn<sup>2+</sup> finger-forming residues are boxed. B, a model of the zinc finger domain of R.KpnI. The protein backbone is shown as a gray ribbon. Side chains of selected functionally important residues are shown in the wire frame representation and labeled. The predicted positions of Zn<sup>2+</sup> and active site metal ion are indicated by balls.

**TABLE 1**

Zn<sup>2+</sup> atomic absorption spectroscopy of R.KpnI

R.KpnI	Sample preparation	Zn <sup>2+</sup>	[Zn <sup>2+</sup> ]/[E]
$\mu\text{M}$		$\mu\text{M}$	
5.0	Chelex-treated	10.32 $\pm$ 0.4	2.16 $\pm$ 0.08
5.0	100 $\mu\text{M}$ ZnCl <sub>2</sub>	19.54 $\pm$ 1.2	3.96 $\pm$ 0.06
5.0	2 mM MgCl <sub>2</sub>	9.45 $\pm$ 0.4	1.92 $\pm$ 0.08
5.0	10 mM EDTA	9.74 $\pm$ 0.4	1.95 $\pm$ 0.0
5.0	8 M urea	0.20 $\pm$ 0.2	0.04 $\pm$ 0.0

(24). Bound Zn<sup>2+</sup> was not replaceable with other metal ions, since even after exhaustive dialysis against a buffer that contained 10 mM MgCl<sub>2</sub>, 2 mol of Zn<sup>2+</sup> were still retained in the protein, indicating that the site was inert to exchange by Mg<sup>2+</sup>. However, when urea-denatured protein was renatured in presence of ZnCl<sub>2</sub>, the zinc content increased to 4 mol/mol of R.KpnI dimer. Dialysis of this preparation in the presence of MgCl<sub>2</sub> resulted in loss of 2 mol of Zn<sup>2+</sup> from R.KpnI, indicating the replacement of two of the four Zn<sup>2+</sup> ions by Mg<sup>2+</sup>. The other 2 mol of tightly bound zinc could not be replaced by Mg<sup>2+</sup>. These results show that R.KpnI monomer possesses two zinc-binding sites; one is replaceable with Mg<sup>2+</sup>, and another one is not (Table 1).

**Role of the Zn<sup>2+</sup> in Structural Integrity**—To define the role of zinc atoms in R.KpnI, we compared the DNA binding and cleavage properties of native, zinc-demetalated (renatured in the absence of Zn<sup>2+</sup>), and zinc-reconstituted enzymes. The zinc-demetalated R.KpnI (the apoenzyme with no Zn<sup>2+</sup> bound) did not bind DNA (Fig. 2A). The enzyme had no DNA cleavage activity in the presence of 2 mM MgCl<sub>2</sub>. Similar experiments were carried out with native and zinc reconstituted R.KpnI (Fig. 2B). The zinc-reconstituted enzyme binds and cleaves the DNA in a promiscuous manner in Mg<sup>2+</sup>-catalyzed reactions, similar to the native enzyme. To investigate whether the loss of DNA binding and cleavage in Zn<sup>2+</sup>-demetalated R.KpnI is due to the structural alterations in the protein, we carried out CD analysis. In presence of Zn<sup>2+</sup>, the far-UV CD spectrum of R.KpnI has two negative maxima at 208 and 222 nm, which is a characteristic of helical conformation. The zinc-demetalated enzyme showed altered secondary structure compared with zinc-re-

constituted enzyme, indicating the importance of Zn<sup>2+</sup> coordination to maintain the secondary structure of the R.KpnI (Fig. 3A). The stability of these proteins was monitored by CD thermal denaturation. Unfolding profiles were measured at 222 nm, from 30 to 75 °C. The *T<sub>m</sub>* of zinc-reconstituted enzyme was increased by ~8 °C over the zinc-demetalated enzyme, indicating a role for Zn<sup>2+</sup> in stability of the enzyme (Fig. 3B). In accordance with CD spectroscopy and thermal melting experiments, proteolytic experiments also showed that the zinc-demetalated enzyme is more susceptible to trypsin cleavage than the native or zinc-reconstituted

enzyme (Fig. 3C). We conclude that Zn<sup>2+</sup> is required for stabilization of the enzymatically active R.KpnI conformation.

**The CCCH Motif Is Involved in Zn<sup>2+</sup> Coordination and Maintenance of the R.KpnI Structure**—To establish that the zinc binding is through the unusual zinc finger motif shown in Fig. 1A, point mutations were generated in R.KpnI. The cysteines (Cys<sup>119</sup>, Cys<sup>128</sup>, and Cys<sup>171</sup>) and histidine (His<sup>174</sup>) of the putative motif were individually changed into alanine by site-directed mutagenesis. The mutant proteins were analyzed for radioactive zinc binding using a zinc blotting assay. All of the alanine replacement mutants failed to bind radioactive zinc (Fig. 4A) in contrast to R.KpnI.

Zn<sup>2+</sup> has been shown to be essential for the folding and stability of many Zn<sup>2+</sup> finger proteins. Zinc blotting experiments indicate that Cys<sup>119</sup>, Cys<sup>128</sup>, Cys<sup>171</sup>, and His<sup>174</sup> are responsible for coordinating Zn<sup>2+</sup> in R.KpnI. We examined the effect of impairment in Zn<sup>2+</sup> coordination on the stability of the enzyme by monitoring the CD thermal melting curves of the alanine replacement mutant proteins. The normalized CD absorbance at 222 nm as a function of temperature for WT and mutants is shown in Fig. 4B. The mutant proteins showed decreased thermal stability compared with that of the WT R.KpnI, indicating that the mutations at the CCCH motif affect the folding of the enzyme. Further, the mutant enzymes showed increased protease susceptibility compared with R.KpnI, confirming the importance of the CCCH motif for the structural stability of the enzyme (Fig. 4C).

**Effect of CCCH Zn<sup>2+</sup> Finger Mutations on DNA Cleavage and Binding**—R.KpnI and its mutants were analyzed for the ability to cleave DNA. Under the assay conditions, wherein pUC18 DNA was completely cleaved by 1 nM WT enzyme, there was no cleavage product observed with all the four mutants even at a 100-fold excess of the enzyme (Fig. 4D). To address the cause for the loss of DNA cleavage observed with the mutants, we analyzed the DNA binding ability of the mutants by electrophoretic mobility shift assay. The mutants failed to bind the DNA containing R.KpnI recognition sequence (Fig. 4E). The mutants showed no detectable DNA binding and cleavage, due to the loss of the structure as observed in CD thermal melting



and proteolytic experiments. These results suggest that the loss of coordination with zinc affected the structural integrity of the protein, concomitantly affecting the activity of the enzyme. The loss of DNA binding and cleavage seen with single amino acid substitution in R.KpnI is a typical characteristic of  $\text{Zn}^{2+}$  finger proteins where  $\text{Zn}^{2+}$  has a structural role.

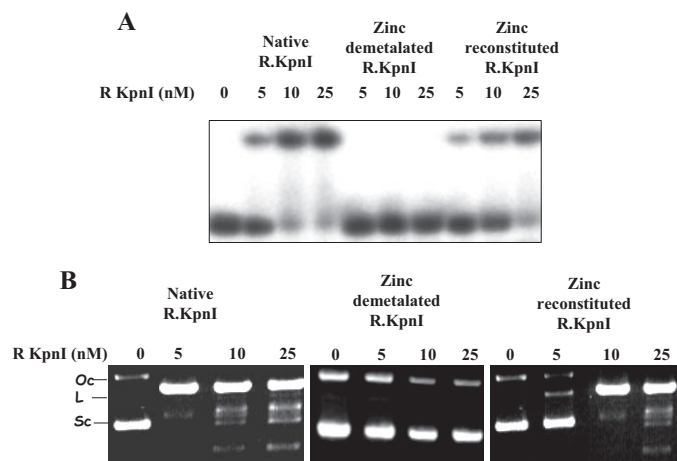


**FIGURE 2. Intrinsically bound zinc ions are essential for DNA binding and  $\text{Mg}^{2+}$ -mediated DNA cleavage.** A, electrophoretic mobility shift assay. Different concentrations of native, zinc-demetalated, and zinc-reconstituted R.KpnI (as indicated) were incubated with  $^{32}\text{P}$ -labeled oligonucleotide containing 5'-GGTACC-3' sequence. The products were analyzed by 8% PAGE and visualized by a PhosphorImager. B, effect of  $\text{Zn}^{2+}$  on DNA cleavage. Native, zinc-demetalated, and zinc-reconstituted R.KpnI (5, 10, and 25 nM) were incubated with 500 ng of pUC18 DNA in the presence of 2 mM  $\text{MgCl}_2$  for 1 h. The reactions were terminated by adding a mixture of 0.6% SDS and 25 mM EDTA. The samples were analyzed on 1.2% agarose gel. SC, L, and OC indicate the positions of the supercoiled, linear, and open circular form of the plasmid, respectively.

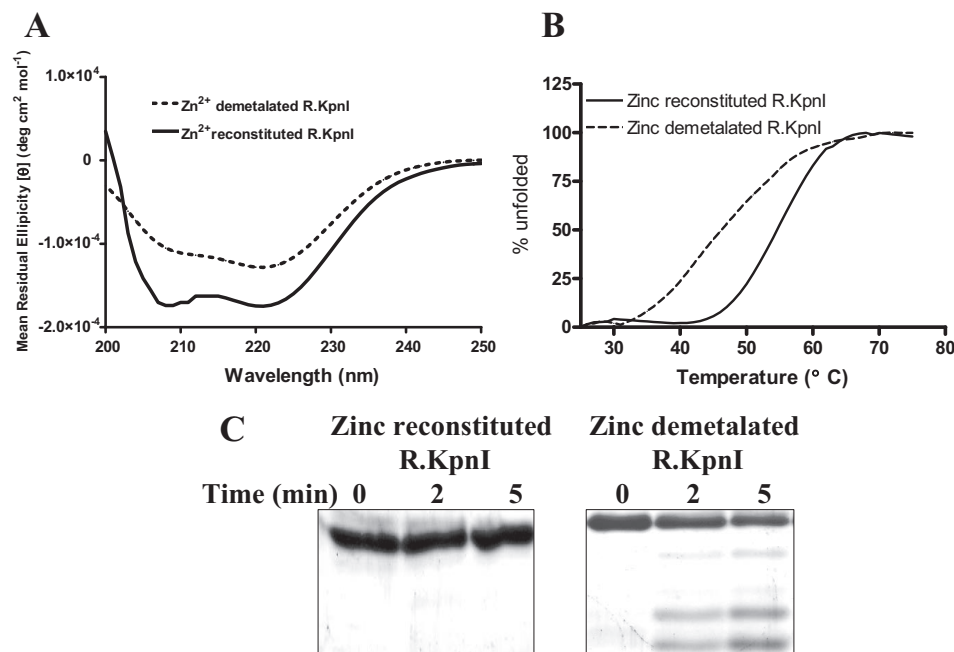


**FIGURE 3. Structural alterations in R.KpnI.** A, CD spectra of R.KpnI. Shown are the mean residue ellipticity of CD spectra for demetallated (dotted line) and zinc-reconstituted R.KpnI (continuous line). Changes in secondary structure were monitored by scanning from 200 to 250 nm. B, temperature-dependent CD measurements (222 nm) for demetallated (dotted line) and zinc-reconstituted R.KpnI (continuous line). All spectra represent the average of three scans using protein concentrations of 0.25 mg/ml. C, trypsin digestion profiles of zinc-reconstituted and zinc-demetalated R.KpnI. The detailed procedure is described under "Experimental Procedures." The digestion profiles were resolved on 12% SDS-PAGE.

**Specific DNA Cleavage and Suppression of  $\text{Mg}^{2+}$ - and  $\text{Mn}^{2+}$ -induced Promiscuous Activity**—The atomic absorption spectroscopy analysis of zinc-reconstituted R.KpnI showed that the enzyme binds 4 mol of zinc (Table 1). Among the 4 mol, only 2 mol can be readily replaced with  $\text{Mg}^{2+}$ . This hints at the possibility of zinc ions binding to the active site to influence the enzymatic properties of R.KpnI in addition to the tight coordination at the CCCH motif. The additional 2 mol of  $\text{Zn}^{2+}$  bound replacing the  $\text{Mg}^{2+}$  may inhibit DNA cleavage. Surprisingly, the enzyme showed efficient DNA cleavage in the presence of 50  $\mu\text{M}$   $\text{Zn}^{2+}$  (Fig. 5A). To evaluate the role of  $\text{Zn}^{2+}$  in the specificity of R.KpnI, we carried out DNA cleavage experiments at higher enzyme concentrations (50–1000 nM) and in the presence of 100  $\mu\text{M}$   $\text{Zn}^{2+}$ . Even at such high concentrations of the enzyme, promiscuous cleavage is not detected, unlike in  $\text{Mg}^{2+}$ -catalyzed reactions (Fig. 5B). In experiments using one of the noncanonical oligonucleotides (GtTACC) as a substrate in the presence of 2 mM  $\text{Mg}^{2+}$  or 100  $\mu\text{M}$   $\text{Zn}^{2+}$ , the cleavage was observed only with  $\text{Mg}^{2+}$ , indicating that the enzyme is highly specific in the presence of  $\text{Zn}^{2+}$  (Fig. 5C). No detectable DNA cleavage was observed in the presence of  $\text{Zn}^{2+}$  with any of the other noncanonical substrates.

In the qualitative experiments described above,  $\text{Zn}^{2+}$ -mediated enzyme activity appeared to be comparable with the activity in the presence of other metal ions. We resorted to kinetic analysis to obtain quantitative information about  $\text{Zn}^{2+}$  DNA cleavage. Kinetic analysis in the presence of  $\text{Zn}^{2+}$  revealed the turnover number ( $k_{\text{cat}}$ ) of the enzyme to be 2.12  $\text{min}^{-1}$ , which is comparable with that of  $\text{Ca}^{2+}$  (2.20  $\text{min}^{-1}$ ), showing that  $\text{Zn}^{2+}$ -mediated DNA cleavage is as efficient as  $\text{Ca}^{2+}$ -dependent cleavage (Table 2) (22). The  $K_m$  of the enzyme for the canonical sequence with  $\text{Zn}^{2+}$  (24 nM) is similar to that of  $\text{Mg}^{2+}$  (22 nM). The ability of  $\text{Zn}^{2+}$  to replace  $\text{Mg}^{2+}$  from the active site and induce specific cleavage suggests that it may suppress the  $\text{Mg}^{2+}$ -mediated promiscuous activity of the enzyme. Results of  $\text{Zn}^{2+}$  chase experiments on  $\text{Mg}^{2+}$ - or  $\text{Mn}^{2+}$ -bound enzyme-DNA complex showed that the  $\text{Mg}^{2+}$ - or  $\text{Mn}^{2+}$ -mediated promiscuous activity was completely suppressed in the presence of 100  $\mu\text{M}$   $\text{Zn}^{2+}$  (Fig. 5D). The ability of different metal ions to bind the active site indicates the plasticity of the active site. Previous studies revealed that R.KpnI utilizes the HNH motif in its reaction mechanism for  $\text{Mg}^{2+}$ /  $\text{Mn}^{2+}$ /  $\text{Ca}^{2+}$ -mediated DNA cleavage. Residues Asp<sup>148</sup>, His<sup>149</sup>, and Gln<sup>175</sup> together form the active site and are essential for  $\text{Mg}^{2+}$  binding and catalysis (20). The active site

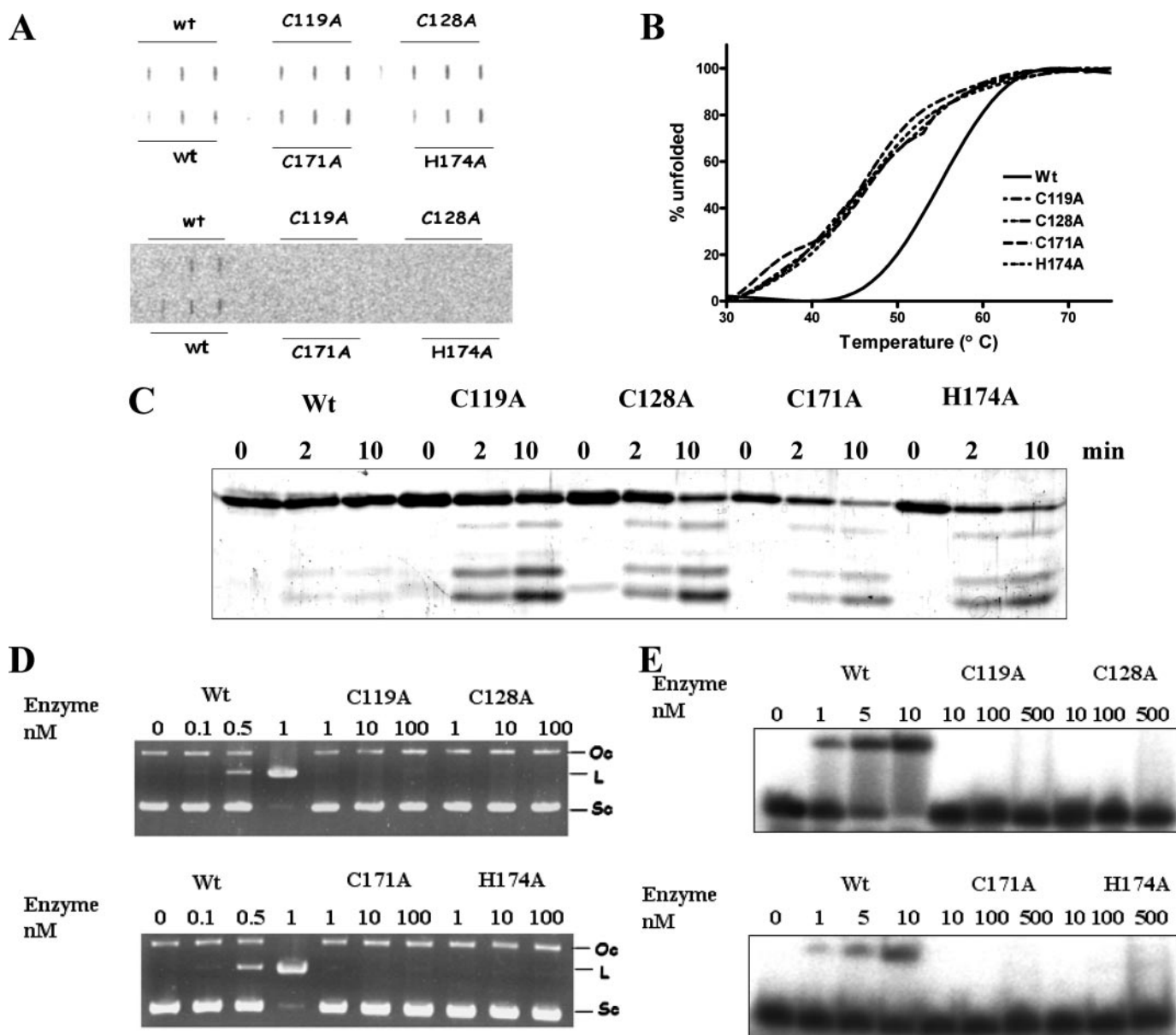


**FIGURE 4. CCCH motif is important for  $Zn^{2+}$  coordination and structural stability of *R. KpnI*.** *A*, analysis of  $^{65}Zn^{2+}$  binding property of the wild type and *R.KpnI* mutants. *R.KpnI* and its CCCH motif mutants (0–6  $\mu$ g) were spotted on nitrocellulose membrane and processed for  $^{65}Zn^{2+}$  binding as described under "Experimental Procedures." *Top*, Ponceau-S-stained membrane, indicating the amounts of transferred protein subsequently used for zinc blot analysis. *Bottom*, blot showing the level of  $^{65}Zn^{2+}$  binding to *R.KpnI*. *B*, the thermal unfolding of the proteins was determined by CD analysis at 222 nm as described under "Experimental Procedures." The melting curves of WT and mutants are shown in different line patterns as indicated. *C*, trypsin digestion profiles of *R.KpnI* and its mutants. Purified and dialyzed proteins were incubated with trypsin at a trypsin/protein ratio (w/w) of 1:200 for 2 and 10 min at 37 °C. The reactions were stopped by the addition of stop buffer. The polypeptide fragments were resolved on 12% SDS-PAGE and stained with Coomassie Blue. *D*, catalytic activities of WT and mutants. The pUC18 containing a single recognition site for *R.KpnI* was incubated with WT (0.1, 0.5, and 1 nM) and CCCH motif mutants (1, 10, and 100 nM) for 60 min at 37 °C. *E*, DNA binding properties of the mutant proteins. WT (1, 5, and 10 nM) and mutant enzymes (10, 100, and 500 nM) were incubated with 3.75 nM  $^{32}P$ -labeled 20-mer duplex oligonucleotide containing recognition sequence (supplementary Table 1) as described under "Experimental Procedures."

mutant enzymes D148G, H149L, and Q175E were analyzed for  $Zn^{2+}$ -mediated DNA cleavage (supplemental Fig. 1).  $Zn^{2+}$ -mediated cleavage also relies on the same catalytic motif, indicating the inherent flexibility of the *R.KpnI* active site HNH motif to accommodate  $Mg^{2+}$ ,  $Mn^{2+}$ ,  $Ca^{2+}$ , and  $Zn^{2+}$ . Replacement of the other metal ions from the active site by  $Zn^{2+}$  and retention of the catalytic activity with kinetic constants comparable with those of  $Mg^{2+}$ ,  $Mn^{2+}$ , and  $Ca^{2+}$  indicate that  $Zn^{2+}$  is a cofactor for *R.KpnI*.

## DISCUSSION

Zinc finger proteins are involved in fundamental cellular processes (*viz.* replication, transcription, repair, translation, and programmed cell death) (7). Zinc finger motifs have also been discovered and implicated in maintenance of the structural architecture in a number of nucleases (9, 14, 26). We demonstrate that a sequence motif ( $^{119}CX_8CX_{42}CX_2H^{174}$ ) found in *R.KpnI* is a zinc binding motif. Based on the conserved arrangements of cysteines and/or histidines, several classes of zinc fin-

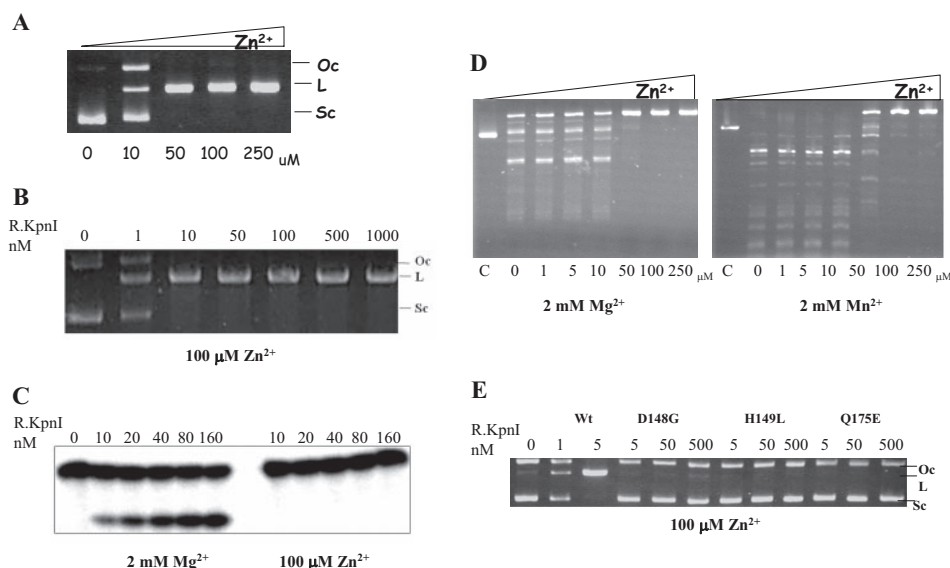


**FIGURE 5. Zn<sup>2+</sup> catalyzed DNA cleavage.** A, zinc-dependent DNA cleavage by R.KpnI. 5 nM R.KpnI was incubated with pUC18 in assay buffer (10 mM Tris-HCl, pH 7.4) containing different concentrations of Zn<sup>2+</sup> (10–250 μM) at 37 °C for 1 h. B and C, high fidelity DNA cleavage in the presence of Zn<sup>2+</sup>. B, 0.5 μg of pUC18 was incubated with R.KpnI (1–1000 nM) in the presence of 100 μM Zn<sup>2+</sup>. C, 5 nM end-labeled noncanonical oligonucleotides (GtTACC) was incubated with increasing concentrations of R.KpnI in the presence of 2 mM Mg<sup>2+</sup> or 100 μM Zn<sup>2+</sup> as indicated. D, effect of Zn<sup>2+</sup> on Mg<sup>2+</sup>- or Mn<sup>2+</sup>-mediated promiscuous activity. pUC18 (1 μg) was incubated with 20 units of R.KpnI in the presence of 2 mM Mg<sup>2+</sup> or 2 mM Mn<sup>2+</sup>, and the reactions were carried out with increasing concentrations of Zn<sup>2+</sup> as indicated. The reactions were terminated by adding a mixture of 0.6% SDS and 25 mM EDTA. The samples were analyzed on 1.2% agarose gel or 10% urea-PAGE. E, analysis of DNA cleavage by active site mutants in the presence of Zn<sup>2+</sup>. WT (1 and 5 nM) and D148G, H149L, and Q175E (5, 50, and 500 nM) mutant proteins were incubated with 0.5 μg of pUC18 DNA in the presence of 100 μM Zn<sup>2+</sup>, and the products were electrophoresed on 1.2% agarose gel.

**TABLE 2**  
Kinetic parameters of R.KpnI with different divalent metal ions

Metal ions	$K_m$	$K_{cat}$	$K_{cat}/K_m$
	<i>M</i>	<i>min</i> <sup>-1</sup>	<i>M</i> <sup>-1</sup> <i>s</i> <sup>-1</sup>
Zn <sup>2+</sup>	24 ± 1.6 × 10 <sup>-9</sup>	2.12 ± 0.16	1.1 ± 0.4 × 10 <sup>6</sup>
Mg <sup>2+</sup> <sup>a</sup>	22 ± 0.8 × 10 <sup>-9</sup>	4.32 ± 0.12	3.2 ± 0.3 × 10 <sup>6</sup>
Mn <sup>2+</sup> <sup>a</sup>	21 ± 1.3 × 10 <sup>-9</sup>	4.62 ± 0.18	3.6 ± 0.4 × 10 <sup>6</sup>
Ca <sup>2+</sup> <sup>a</sup>	36 ± 1.6 × 10 <sup>-9</sup>	2.20 ± 0.18	1.0 ± 0.1 × 10 <sup>6</sup>

<sup>a</sup> Kinetic constants obtained from Saravanan *et al.* (22).

ger families (CCHH, CCCC, CCHC, and CHCC), have been characterized and shown to be involved in interactions with DNA, RNA, or other proteins (27). CCCH-type zinc fingers were identified in a number of RNA-binding proteins of eukaryotic origin (28) and also found in Mcm10 protein, which is essential for the formation of active homocomplex (29). The arrangement of three cysteines and a histidine in the CCCH zinc finger found in R.KpnI is rare in prokaryotic proteins. The CCCH zinc fingers were identified in replication protein A homologues in different lineages of Euryarchaeota (30), RPA41 from *Pyrococcus furiosus* (31) and 50 S ribosomal protein L36 from *Thermus thermophilus* (32).

R.KpnI thus is a new member of the CCCH Zn<sup>2+</sup> finger family and is the first REase to have this motif. The Zn<sup>2+</sup> fingers in other members having this motif listed above have varied roles in protein-protein interactions, protein-nucleic acid interactions, structural integrity, and folding. From the results presented in Fig. 2, it is clear that tightly bound Zn<sup>2+</sup> has a structural role, since it supports Mg<sup>2+</sup>-mediated promiscuous cleavage. The second Zn<sup>2+</sup> atom, which is loosely bound to the active site, imparts catalytic function. A peculiar characteristic

of R.KpnI is its highly promiscuous behavior in the presence of Mg<sup>2+</sup> not seen with any other REase (21). The Mg<sup>2+</sup> (and Mn<sup>2+</sup>)-mediated promiscuous cleavage by R.KpnI is completely suppressed by Zn<sup>2+</sup> meanwhile, inducing the high fidelity cleavage. The architectural plasticity of the R.KpnI active site allows the binding of Mg<sup>2+</sup>, Mn<sup>2+</sup>, Ca<sup>2+</sup>, or Zn<sup>2+</sup>, which have different coordination chemistry and geometry to induce promiscuous or specific cleavage. Thus, in R.KpnI, Zn<sup>2+</sup> has both structural and catalytic roles, together not found in any enzyme so far. The tightly bound Zn<sup>2+</sup> at the CCCH motif imparts structural integrity for the enzyme, whereas the readily exchangeable Zn<sup>2+</sup> at the active site induces high specificity cleavage.

Finally, Zn<sup>2+</sup> finger motifs as such appear to be extremely rare in nucleases of prokaryotic origin. Although the HNH motif is commonly found in diverse classes of nucleases, the zinc finger motifs are

found only in McrA, I-PpoI, and T4 endonuclease VII belonging to the superfamily. Although the Cys<sub>4</sub> zinc finger of T4 endonuclease VII has a structural role, the function of similar zinc finger in McrA is not known. The two Zn<sup>2+</sup> fingers (CCCH and CCHC) in I-PpoI are also important for structural stabilization of the protein core. The catalytic and structural role for Zn<sup>2+</sup> in R.KpnI hints at its distant origin and possibly additional yet unknown function in *Klebsiella pneumoniae*.

**Acknowledgments**—We thank J. M. Bujnicki for the R.KpnI modeling and the Departments of Biochemistry and Molecular Biophysics and Solid State Chemistry Units for circular dichroism, fluorometry, and atomic absorption spectrometry, respectively.

## REFERENCES

- Coleman, J. E. (1992) *Annu. Rev. Biochem.* **61**, 897–946
- Vallee, B. L., and Auld, D. S. (1990) *Biochemistry* **29**, 5647–5659
- Keilin, D., and Mann, T. (1940) *Biochem. J.* **34**, 1163–1176
- Hanas, J. S., Hazuda, D. J., Bogenhagen, D. F., Wu, F. Y., and Wu, C. W. (1983) *J. Biol. Chem.* **258**, 14120–14125
- Miller, J., McLachlan, A. D., and Klug, A. (1985) *EMBO J.* **4**, 1609–1614
- Sankaranarayanan, R., Dock-Bregeon, A. C., Rees, B., Bovee, M., Caillet, J., Romby, P., Francklyn, C. S., and Moras, D. (2000) *Nat. Struct. Biol.* **7**, 461–465
- Laity, J. H., Lee, B. M., and Wright, P. E. (2001) *Curr. Opin. Struct. Biol.* **11**, 39–46
- Flick, K. E., Jurica, M. S., Monnat, R. J., Jr., and Stoddard, B. L. (1998) *Nature* **394**, 96–101
- Van Roey, P., Waddling, C. A., Fox, K. M., Belfort, M., and Derbyshire, V. (2001) *EMBO J.* **20**, 3631–3637
- Hosfield, D. J., Guan, Y., Haas, B. J., Cunningham, R. P., and Tainer, J. A. (1999) *Cell* **98**, 397–408

11. Ko, T. P., Liao, C. C., Ku, W. Y., Chak, K. F., and Yuan, H. S. (1999) *Structure* **7**, 91–102
12. Gite, S., and Shankar, V. (1992) *Eur. J. Biochem.* **210**, 437–441
13. Bujnicki, J. M., Radlinska, M., and Rychlewski, L. (2000) *Mol. Microbiol.* **37**, 1280–1281
14. Vanamee, E. S., Hsieh, P., Zhu, Z., Yates, D., Garman, E., Xu, S., and Aggarwal, A. K. (2003) *J. Mol. Biol.* **334**, 595–603
15. Roberts, R. J., Vincze, T., Posfai, J., and Macelis, D. (2007) *Nucleic Acids Res.* **35**, D269–D270
16. Pingoud, A., Fuxreiter, M., Pingoud, V., and Wende, W. (2005) *Cell Mol. Life Sci.* **62**, 685–707
17. Sapranaukas, R., Sasnauskas, G., Lagunavicius, A., Vilkaitis, G., Lubys, A., and Siksnys, V. (2000) *J. Biol. Chem.* **275**, 30878–30885
18. Aravind, L., Makarova, K. S., and Koonin, E. V. (2000) *Nucleic Acids Res.* **28**, 3417–3432
19. Bujnicki, J. M., Radlinska, M., and Rychlewski, L. (2001) *Trends Biochem. Sci.* **26**, 9–11
20. Saravanan, M., Bujnicki, J. M., Cymerman, I. A., Rao, D. N., and Nagaraja, V. (2004) *Nucleic Acids Res.* **32**, 6129–6135
21. Chandrashekar, S., Saravanan, M., Radha, D. R., and Nagaraja, V. (2004) *J. Biol. Chem.* **279**, 49736–49740
22. Saravanan, M., Vasu, K., Kanakaraj, R., Rao, D. N., and Nagaraja (2007) *Nucleic Acids Res.* **35**, 2777–2786
23. Kirsch, R. D., and Joly, E. (1998) *Nucleic Acids Res.* **26**, 1848–1850
24. Chandrashekar, S., Babu, P., and Nagaraja, V. (1999) *J. Biosci.* **24**, 269–277
25. Bradford, M. M. (1976) *Anal. Biochem.* **72**, 248–254
26. Raaijmakers, H., Vix, O., Toro, I., Golz, S., Kemper, B., and Suck, D. (1999) *EMBO J.* **18**, 1447–1458
27. Berg, J. M., and Godwin, H. A. (1997) *Annu. Rev. Biophys. Biomol. Struct.* **26**, 357–371
28. Amann, B. T., Worthington, M. T., and Berg, J. M. (2003) *Biochemistry* **42**, 217–221
29. Cook, C. R., Kung, G., Peterson, F. C., Volkman, B. F., and Lei, M. (2003) *J. Biol. Chem.* **278**, 36051–36058
30. Lin, Y., Robbins, J. B., Nayannor, E. K. D., Chen, Y. H., and Cann, I. K. O. (2005) *J. Bacteriol.* **187**, 7881–7889
31. Komori, K., and Ishino, Y. (2001) *J. Biol. Chem.* **276**, 25654–25660
32. Boysen, R. I., and Hearn, M. W. (2001) *J. Pept. Res.* **57**, 19–28
33. Sambrook, J., Fritsch, E. F., and Maniatis, T. (1989) *Molecular Cloning: A Laboratory Manual*, 2nd Ed., Cold Spring Harbor Laboratory, Cold Spring Harbor, NY